RESEARCH PAPER

Quality By Design Based Development And Optimization Of Green Synthesis Of Silver Nanoparticles Incorporated Into Chitosan Hydrogel: Physicochemical Characterization

Indu R S[1], P Shanmugasundaram[2*]

[1]PhD Research Scholar. Department of Pharmaceutics, School of Pharmaceutical Sciences, Vels institute of Science, Technology and Advanced Studies, Pallavaram, Chennai

[2]Dean, Department of Pharmaceutical Sciences, Vels institute of Science, Technology and Advanced Studies, Pallavaram, Chennai*

ABSTRACT

The present study aimed to develop and optimize green-synthesized silver nanoparticles (AgNPs) incorporated into a chitosan hydrogel using a Quality by Design (QbD) approach for potential wound-healing applications. Neem (*Azadirachta indica*) leaf extract was employed as a natural reducing and stabilizing agent for the eco-friendly synthesis of AgNPs. A Box–Behnken Design (BBD) was utilized to evaluate the effects of silver nitrate concentration, neem extract concentration, and pH on critical quality attributes, including particle size, zeta potential, and polydispersity index (PDI). The optimized formulation was obtained at 0.5336% silver nitrate concentration, 1.35% neem extract concentration, and pH 7.04, yielding nanoparticles with a particle size of 36.8 nm, zeta potential of −10.40mV, and PDI of 0.262. Characterization studies using UV–Visible spectroscopy, FTIR, XRD, SEM, and EDX confirmed the successful synthesis of stable, crystalline silver nanoparticles. The optimized AgNPs were incorporated into a chitosan hydrogel and further characterized for physicochemical and morphological properties. SEM analysis revealed a porous hydrogel network with uniformly distributed silver nanoparticles, while FTIR and XRD studies confirmed successful incorporation within the polymeric matrix. The QbD-based optimization approach demonstrated excellent predictive capability and reproducibility. The developed AgNP-loaded chitosan hydrogel represents a promising, environmentally sustainable platform for topical wound-healing applications with potential antimicrobial and tissue-regenerative benefits.

Keywords: Quality by Design, Silver Nanoparticles, Green Synthesis, Neem Extract, Chitosan Hydrogel, Box–Behnken Design, in Physicochemical characterization.

How to site this article : Indu RS, Shanmugasundaram P. Quality By Design Based Development And Optimization Of Green Synthesis Of Silver Nanoparticles Incorporated Into Chitosan Hydrogel: Physicochemical Characterization. Int J Drug Deliv Technol.2026;16(64s):1183-1202.DOI: 10.25258/ijddt.16.64s.126

INTRODUCTION

The management of wound infections remains a critical challenge due to the increasing prevalence of antimicrobial resistance, prolonged inflammation, and delayed tissue regeneration. Conventional topical therapies often fail to provide sustained antimicrobial action and adequate healing support, necessitating the development of advanced multifunctional delivery systems[1,2]. In recent years, nanotechnology-based approaches have gained significant attention for wound healing applications due to their ability to enhance drug stability, controlled release, and targeted action[3,4,5]. Among these, silver nano particles have been extensively studied for their potent broad-spectrum antimicrobial activity, acting through disruption of microbial membranes, generation of reactive oxygen species, and inhibition of cellular functions.

However, conventional chemical synthesis of silver nanoparticles involves toxic reagents and harsh conditions, raising concerns regarding safety and environmental impact. To overcome these limitations, green synthesis of silver nanoparticles has emerged as a sustainable and eco-friendly alternative[6,7,8]. This approach utilizes plant extracts and natural biomolecules as reducing and stabilizing agents, eliminating the need for hazardous chemicals. Green-synthesized nanoparticles have been reported to exhibit enhanced antimicrobial, antioxidant, and anti-inflammatory properties, making them highly suitable for wound healing applications[9.10.11]. Furthermore, recent studies have demonstrated that plant-based green synthesized silver nanoparticles significantly improve wound healing outcomes due to their synergistic biological activities.

Chitosan, a biodegradable and biocompatible cationic polymer, has been extensively investigated as a drug delivery carrier due to its inherent antimicrobial activity, bioadhesive nature, and excellent film-forming properties. Chitosan-based hydrogels are particularly advantageous for topical applications as

they maintain a moist wound environment, enhance drug retention, and facilitate sustained release[12,13,14]. Recent studies have shown that hydrogels incorporating green-synthesized silver nanoparticles exhibit improved swelling behavior, mechanical strength, and significant antibacterial activity against common wound pathogens, while maintaining low cytotoxicity. Additionally, systematic reviews highlight that silver nanoparticle-loaded hydrogels represent promising alternatives to conventional antibiotics for treating resistant infections[15,63,17,18,19,20]. However, the development of such complex systems requires a systematic and robust approach to ensure consistent quality and performance.

The application of Quality by Design (QbD) principles provides a scientific framework for the development and optimization of pharmaceutical formulations. QbD involves the identification of critical quality attributes (CQAs), critical material attributes (CMAs), and critical process parameters (CPPs), along with the use of design of experiments (DoE) to establish a design space. This approach ensures reproducibility, efficiency, and regulatory compliance while minimizing variability in the final product. Therefore, the present study aims to develop and optimize green-synthesized silver nanoparticles incorporated into a chitosan-based hydrogel using a QbD framework. The study focuses on understanding the influence of formulation variables on key quality attributes and evaluating the system for preparation of green synthesis silver nanoparticles, thereby providing a promising platform for next-generation topical drug delivery systems.

MATERIALS & METHODS

MATERIALS

Silver nitrate ($AgNO_3$) was used as the silver precursor, and fresh neem (*Azadirachta indica*) leaves were used for the preparation of the aqueous extract. Chitosan was employed as the hydrogel-forming polymer, while glacial acetic acid and sodium tripolyphosphate (TPP) were used for polymer dissolution and cross-linking, respectively. Distilled water was used throughout the study. All chemicals and reagents were of analytical grade and used as received.

METHODS

Preparation of Neem Extract

Fresh and healthy leaves of neem (*Azadirachta indica*) were collected, washed thoroughly with running tap water followed by distilled water to remove dust and impurities, and shade-dried at room temperature for 7–10 days. The dried leaves were pulverized using a mechanical grinder and passed through a suitable sieve to obtain a uniform powder[21,22.]. For the preparation of aqueous neem extract, 10 g of powdered neem leaves were mixed with 100 mL of distilled water and heated at 60–80 °C for 30 minutes under continuous stirring. The mixture was allowed to cool to room temperature and filtered initially through muslin cloth followed by Whatman No. 1 filter paper to remove particulate matter. The obtained filtrate was collected and stored at 4 °C until further use. The freshly prepared extract was used as a reducing and stabilizing agent for the green synthesis of silver nanoparticles.

Procedure for QbD-Guided Green Synthesis of Silver Nanoparticles

Green-synthesized silver nanoparticles (AgNPs) were prepared using a plant extract of Neem as a reducing and stabilizing agent. Initially, a specified concentration of silver nitrate ($AgNO_3$) solution was prepared using distilled water. The plant extract was filtered and added dropwise to the $AgNO_3$ solution under continuous stirring. The reaction mixture was maintained at a controlled temperature and pH to facilitate the reduction of silver ions into nanoparticles. The formation of AgNPs was confirmed by a color change (pale yellow to brown) and further verified using UV–Visible spectroscopy. The synthesized nanoparticles were centrifuged, washed, and dried for further characterization. A Quality by Design (QbD) approach was employed to systematically optimize the formulation variables[23,24,25]. Critical material attributes such as $AgNO_3$ concentration, plant extract concentration, and pH were identified, while particle size, polydispersity index, and zeta potential were considered as critical quality attributes. A Box–Behnken design (BBD) was used to evaluate the influence of selected variables and to establish an optimized formulation with desired nanoparticle characteristics.

Table 01. Box–Behnken Design Matrix for Green Synthesis of Silver Nanoparticles

Factors and Levels

Factor	**Code**	**Low (-1)**	**Medium (0)**	**High (+1)**
Ag concentration (%)	X1	0.5	1.0	1.5
Plant extract (%)	X2	1	3	5
pH	X3	5	7	9
Responses				
Particle size (nm)	Y1	Minimize		
Polydispersity index	Y2	Minimize		
Zeta potential (mV)	Y3	Within range ±20		

Table 02. Box–Behnken Design Matrix with Responses for Green Synthesis of Silver Nanoparticles

	Factor 1	Factor 2	Factor 3	Response 1	Response 2	Response 3
Run	**A:Ag Con.**	**B:Extract Con.**	**C:pH**	**Particle size**	**Zeta Potential**	**PDI**
	%	**%**		**nm**	**mV**	
1	1	3	8	55.067	-13.65	0.423
2	1	5	9	59	-25.22	1.116
3	0.5	3	9	35.64	-18.68	1.063
4	1	3	8	56.032	-13.36	0.419
5	1	1	9	62.06	-9.09	0.925
6	1	1	7	60.04	-7.65	0.311
7	1.5	3	7	72.37	-1.68	0.108
8	0.5	1	8	30.05	-6.89	0.607
9	1	3	8	55.53	-11.89	0.458
10	0.5	3	7	36.07	-13.47	0.139
11	1	5	7	58.42	-16.38	0.155
12	0.5	5	8	37.51	-22.88	0.693
13	1	3	8	52.07	-10.6	0.403
14	1.5	5	8	50.07	-10.2	0.602
15	1.5	3	9	69.06	-16.21	0.953
16	1.5	1	8	70.08	-0.65	0.613
17	1	3	8	50.36	-11.2	0.442

Preparation of Silver Nanoparticles Incorporated Chitosan-Based Hydrogel

Silver nanoparticles (AgNPs) were incorporated into a chitosan-based hydrogel following a previously reported method with slight modifications. Briefly, chitosan was dissolved in 1% (v/v) acetic acid under continuous stirring to obtain a clear polymeric solution. Separately, the preformed green-synthesized silver nanoparticles were dispersed in distilled water and sonicated to ensure uniform distribution.

The nanoparticle dispersion was then slowly added to the chitosan solution under constant stirring to achieve homogeneous mixing. To enhance gel formation and stability, a suitable cross-linking agent such as sodium tripolyphosphate (TPP) or a neutralizing agent was added dropwise. The mixture was stirred until a uniform hydrogel was formed with appropriate viscosity.

The prepared hydrogel was allowed to stand to remove entrapped air bubbles and then stored in airtight containers for further evaluation. The formulation was subsequently characterized for pH, viscosity, spreadability, drug content.

Characterization of green synthesis of silver nanoparticles

The green synthesis of silver nanoparticles (AgNPs) was carried out using neem (*Azadirachta indica*) leaf extract as a reducing and stabilizing agent. The synthesized nanoparticles were characterized using various analytical techniques to evaluate their

physicochemical properties, morphology, crystallinity, elemental composition, and stability.

1. Particle Size and Polydispersity Index (PDI)

The average particle size and polydispersity index (PDI) of the synthesized silver nanoparticles were determined using Dynamic Light Scattering (DLS). The nanoparticle suspension was appropriately diluted with distilled water to avoid multiple scattering effects and analyzed at room temperature. Particle size analysis provides information regarding the hydrodynamic diameter of the nanoparticles, while the PDI indicates the uniformity of particle size distribution. Lower PDI values correspond to a more homogeneous nanoparticle population.

2. Zeta Potential Analysis

The surface charge and colloidal stability of the silver nanoparticles were evaluated using a zeta potential analyzer. The nanoparticle dispersion was diluted with deionized water and analyzed at room temperature. Zeta potential measurements provide insight into the electrostatic repulsion between particles and their tendency to remain dispersed or aggregate during storage.

3. Morphological Analysis by Scanning Electron Microscopy (SEM)

The morphology, size, and surface characteristics of the synthesized silver nanoparticles were examined using Scanning Electron Microscopy (SEM). A drop of the nanoparticle suspension was placed on a suitable substrate and dried under vacuum. The dried sample was sputter-coated with a thin layer of gold and observed under different magnifications. SEM images were used to determine particle shape, surface texture, and aggregation behavior.

4. Fourier Transform Infrared Spectroscopy (FTIR)

Fourier Transform Infrared Spectroscopy (FTIR) was performed to identify the functional groups present in the neem extract and their involvement in the reduction and stabilization of silver nanoparticles. Dried samples of neem extract and synthesized AgNPs were scanned over the range of 4000–400 cm^{-1}. Characteristic absorption bands corresponding to hydroxyl, carbonyl, amine, and phenolic groups were analyzed to investigate the interaction between phytoconstituents and silver nanoparticles.

5. X-ray Diffraction (XRD)

X-ray diffraction analysis was carried out to determine the crystalline nature of the synthesized silver nanoparticles. Dried nanoparticle samples were scanned over an appropriate 2θ range using Cu-Kα radiation. The diffraction peaks obtained were compared with standard silver diffraction patterns to confirm the formation of crystalline metallic silver and estimate crystallite characteristics.

6. UV–Visible Spectroscopy

UV–Visible spectroscopic analysis was performed to confirm the formation of silver nanoparticles. The reaction mixture was scanned in the wavelength range of 200–800 nm using a UV–Visible spectrophotometer. The appearance of a characteristic surface plasmon resonance (SPR) peak between 400 and 450 nm. Changes in peak position and intensity were used to assess nanoparticle formation and stability.

7. Energy-Dispersive X-ray Spectroscopy (EDX)

Energy-dispersive X-ray spectroscopy (EDX) analysis was performed to determine the elemental composition of the synthesized nanoparticles. The sample was mounted on a conductive stub and analyzed using an EDX detector coupled with a scanning electron microscope operated at an accelerating voltage of 15 kV. Characteristic X-rays emitted from the sample were recorded and analyzed to identify the elemental constituents. The presence of a strong silver signal confirmed the successful synthesis of silver nanoparticles, while additional signals corresponding to carbon and oxygen were attributed to phytochemical compounds from the neem extract that acted as reducing and capping agents.

Section 8: Hydrogel Preparation

The optimized silver nanoparticles (AgNPs) synthesized using neem extract were incorporated into a chitosan-based hydrogel system to improve topical retention, ease of application, and sustained release characteristics. Chitosan was dispersed in 1% (v/v) acetic acid solution under continuous magnetic stirring until a clear and homogeneous gel was obtained. The prepared silver nanoparticle suspension was then added slowly to the polymeric solution under constant stirring to ensure uniform distribution throughout the hydrogel matrix. The mixture was stirred for an additional period until a smooth and homogeneous hydrogel was formed. The final formulation was stored in airtight containers at room temperature until further characterization. The prepared hydrogel was visually inspected for homogeneity, appearance, and the absence of phase separation or particulate matter.

Section 9: Hydrogel Characterization

Scanning Electron Microscopy (SEM)

The surface morphology of the silver nanoparticle-loaded chitosan hydrogel was examined using Scanning Electron Microscopy (SEM). The hydrogel sample was freeze-dried and mounted on an aluminum stub using double-sided conductive carbon tape. The sample surface was sputter-coated with a thin layer of gold to improve conductivity. SEM analysis was performed at different magnifications under suitable accelerating voltage conditions. The micrographs obtained were used to evaluate the surface characteristics, porosity, and distribution of silver nanoparticles within the chitosan hydrogel matrix.

10. Fourier Transform Infrared Spectroscopy (FTIR)

FTIR spectroscopy was carried out to identify the functional groups and investigate the interactions between chitosan and silver nanoparticles. The dried hydrogel sample was mixed with potassium bromide (KBr) and compressed into pellets. The spectra were recorded over the range of 4000–400 cm^{-1} using an FTIR spectrophotometer. The characteristic absorption bands were analyzed to confirm the presence of chitosan functional groups and possible interactions responsible for the stabilization and incorporation of silver nanoparticles within the hydrogel network.

11.X-Ray Diffraction (XRD)

The crystalline nature of the silver nanoparticle-loaded chitosan hydrogel was analyzed using X-ray Diffraction (XRD). The dried hydrogel sample was finely powdered and subjected to XRD analysis using Cu-Kα radiation (λ = 1.5406 Å). The diffraction patterns were recorded over a 2θ range of 10°–80° at a suitable scanning rate. The obtained diffractograms were evaluated to identify the characteristic diffraction peaks of silver nanoparticles and to determine their crystalline structure and successful incorporation into the chitosan hydrogel matrix.

RESULTS AND DISCUSSION

Model Fitting and Statistical Analysis

The Quality by Design (QbD)-based optimization of green synthesized silver nanoparticles (AgNPs) using neem extract was successfully performed using a quadratic response surface model. The independent variables selected were silver nitrate concentration (A), neem extract concentration (B), and pH (C), while particle size, zeta potential, and polydispersity index (PDI) were considered as critical quality attributes (CQAs).

The ANOVA results demonstrated that all three response models were significant, indicating that the selected factors adequately explained the variability in nanoparticle characteristics. Furthermore, the lack-of-fit values for particle size ($p = 0.2166$), zeta potential ($p = 0.1870$), and PDI ($p = 0.0768$) were non-significant, confirming the suitability and reliability of the developed quadratic models for prediction within the design space.

Effect of Formulation Variables on Particle Size

Particle size is a critical parameter affecting nanoparticle stability, cellular uptake, and biological activity. The particle size model was highly significant ($F = 25.88$, $p = 0.0001$).

The polynomial equation obtained was:

Particle Size = 537.458 + 152.145A -21.9512B -0.02125C -68.5775AB -7.2775AC -2.5BC -66.554A^2 -1.6565B^2 +61.6985C^2

Among the studied factors, silver nitrate concentration (A) exerted the most significant effect on particle size ($p < 0.0001$). The positive coefficient (+152.145) indicates that increasing $AgNO_3$ concentration increased particle size. Higher silver ion availability may promote rapid nucleation followed by particle growth and aggregation, resulting in larger nanoparticles. Neem extract concentration (B) showed a negative coefficient (-21.95), suggesting a tendency toward particle size reduction with increasing extract concentration, although the effect was statistically non-significant ($p = 0.0949$). This may be attributed to the increased availability of phytochemicals such as flavonoids, terpenoids, and polyphenols that act as reducing and capping agents, preventing particle agglomeration. The effect of pH was statistically insignificant ($p = 0.9986$); however, the significant quadratic term (C^2, $p = 0.0056$) indicated curvature in the response, suggesting that extreme pH conditions may favor particle enlargement. A significant interaction was observed between silver concentration and extract concentration (AB; $p = 0.0037$), demonstrating that the influence of silver ions on particle size depends on the availability of reducing phytochemicals. The significant quadratic effect of silver concentration (A^2; $p = 0.0038$) further indicates a non-linear relationship between $AgNO_3$ concentration and nanoparticle growth. The optimized formulation produced nanoparticles with an observed particle size of 36.8 nm, which closely matched the predicted value of 34.99 nm, confirming model adequacy.

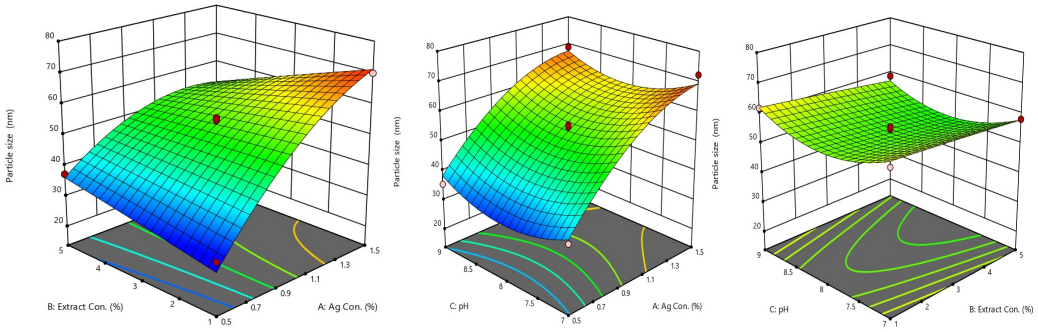

Figure 01. Effect of Formulation Variables on Silver Nanoparticle Size and Stability

The response surface plots demonstrated that silver nitrate concentration (A) had the greatest influence on particle size. Increasing $AgNO_3$ concentration significantly increased particle size from approximately 30 nm to 70 nm, as confirmed by the high F-value (178.93, $p < 0.0001$). This may be due to increased silver ion availability leading to enhanced particle growth and aggregation. Neem extract concentration (B) showed a slight reduction in particle size with increasing concentration. The phytochemicals present in neem extract act as reducing and capping agents, preventing nanoparticle agglomeration and promoting smaller particle formation. The effect of pH (C) was mainly quadratic, with minimum particle size observed at intermediate pH values (around 7.5–8.0). Both lower and higher pH conditions resulted in larger particles, likely due to changes in phytochemical ionization and stabilization efficiency. The perturbation plot revealed that particle size was most sensitive to $AgNO_3$ concentration, followed by pH, while extract concentration showed the least effect. The significant AB interaction ($p = 0.0037$) indicated that the effect of silver concentration depended on the amount of neem extract present. The response surface analysis confirmed that moderate silver concentration, higher extract concentration, and near-neutral pH favor the formation of smaller and more stable neem-mediated silver nanoparticles.

Effect of Formulation Variables on Zeta Potential

Zeta potential is an important indicator of colloidal stability, with higher absolute values indicating stronger electrostatic repulsion between particles. The quadratic model for zeta potential was highly significant ($F = 24.14$, $p = 0.0002$). The developed equation was:

Zeta Potential = -12.14 +4.1475A -6.3B -3.7525C +1.61AB -2.33AC -1.85BC +2.03A^2 -0.045B^2 -2.4C^2

All three main factors significantly influenced zeta potential. Extract concentration (B) exhibited the strongest effect ($F = 105.61$, $p < 0.0001$), followed by silver concentration (A) and pH (C). The negative coefficient of extract concentration (-6.3) indicates that increasing neem extract concentration produced more negative zeta potential values. This observation may be attributed to the adsorption of negatively charged phytoconstituents on the nanoparticle surface, enhancing electrostatic stabilization. Similarly, increasing pH resulted in more negative zeta potential values due to increased ionization of phenolic and carboxylic groups present in neem phytochemicals. The AC interaction ($p = 0.0312$) was significant, indicating that the combined effect of silver concentration and pH influenced nanoparticle surface charge.

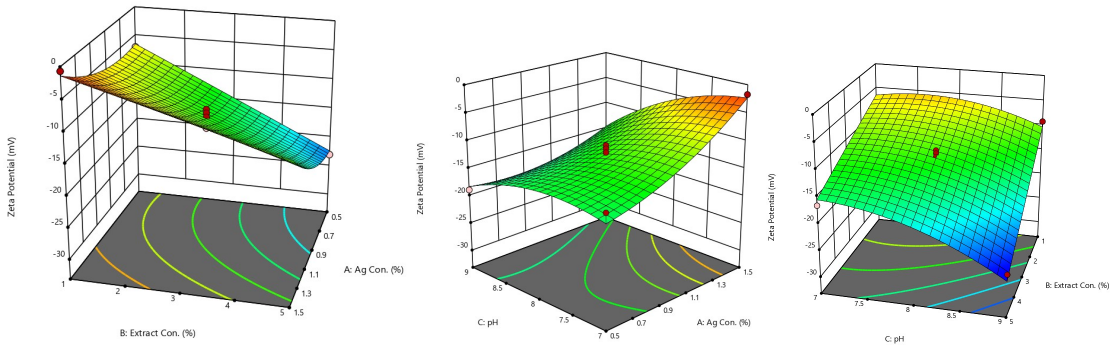

Figure 02. Influence of $AgNO_3$, Neem Extract, and pH on Zeta Potential green synthesized silver nanoparticles.

The response surface analysis revealed that silver nitrate concentration, neem extract concentration, and pH significantly influenced the zeta potential of the synthesized silver nanoparticles. The interaction between silver nitrate concentration and extract concentration showed that increasing both variables resulted in a gradual decrease in zeta potential from approximately −3 mV to −15 mV, indicating enhanced nanoparticle stability. The interaction between silver nitrate concentration and pH demonstrated that higher pH values promoted more negative zeta potential values, while lower pH conditions produced less negative values, suggesting that pH plays an important role in modifying the surface charge of the nanoparticles. The combined effect of extract concentration and pH exhibited the strongest influence on zeta potential, with increasing extract concentration and alkaline pH resulting in zeta potential values approaching −30 mV. This increase in negative surface charge can be attributed to the adsorption of phytochemicals from neem extract onto the nanoparticle surface, providing effective capping and stabilization. The optimized formulation exhibited an observed zeta potential of −10.4 mV, which was in close agreement with the predicted value of −10.74 mV, confirming the adequacy and reliability of the optimization model. Overall, the results indicate that extract concentration and pH had the greatest impact on nanoparticle stability, while their interaction contributed significantly to the development of a more stable colloidal system with reduced aggregation[26,27,28].

Effect of Formulation Variables on Polydispersity Index (PDI)

PDI reflects the uniformity of particle size distribution, where lower values indicate greater homogeneity. The ANOVA analysis showed a significant quadratic model ($F = 8.65$, $p = 0.0048$). The fitted equation was:

PDI = 0.642 +0.351625A +0.1085B -0.004875C -0.05575AB +0.1425AC -0.09675BC +0.5435A^2 +0.26025B^2 +0.023C^2

Silver concentration (A) significantly influenced PDI ($p = 0.0012$). The positive coefficient indicates that increasing silver concentration increased size heterogeneity, likely due to uncontrolled particle growth and aggregation at higher precursor concentrations. The quadratic terms A^2 ($p = 0.0006$) and B^2 ($p = 0.0265$) were significant, indicating nonlinear effects of silver nitrate and neem extract concentrations on particle distribution. These findings suggest that both insufficient and excessive concentrations of reducing agents can adversely affect nanoparticle uniformity.

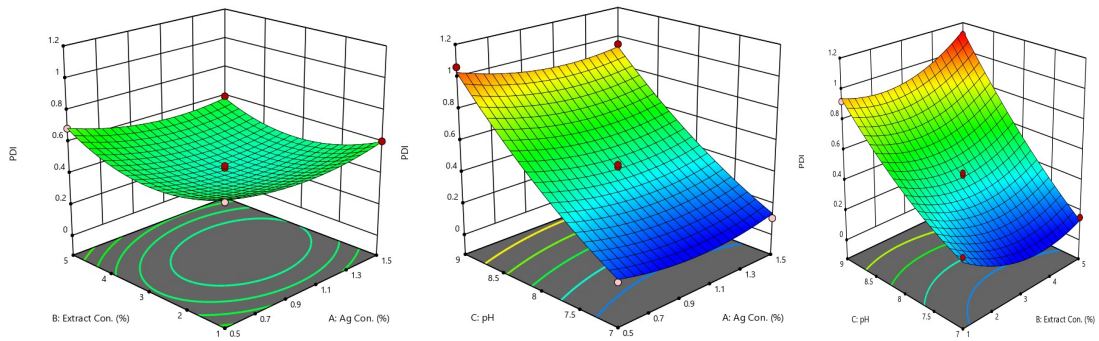

Figure 03. Response surface analysis demonstrated that silver nitrate concentration (A), neem extract concentration (B), and pH (C) significantly influenced the PDI of the Nanoparticles.

The Polydispersity Index (PDI) was employed as a critical quality attribute (CQA) to evaluate the uniformity of particle size distribution in the green-synthesized silver nanoparticles (AgNPs). Response surface analysis demonstrated that silver nitrate concentration (A), neem extract concentration (B), and pH (C) significantly influenced the PDI of the formulation. The interaction between silver nitrate concentration and neem extract concentration showed that moderate levels of both factors favored the formation of nanoparticles with lower PDI values. An adequate amount of plant extract provided sufficient phytoconstituents to reduce and stabilize silver ions, thereby minimizing particle aggregation and promoting a more homogeneous nanoparticle population. Conversely, excessive silver ion concentration increased particle collision and growth, resulting in broader size distributions. The combined effect of silver concentration and pH indicated that higher silver concentrations tended to increase PDI values irrespective of pH, whereas mildly alkaline conditions improved nanoparticle stability. Alkaline pH enhances the ionization of phenolic and flavonoid compounds present in the extract, facilitating rapid reduction of Ag^{+} ions and effective surface capping of the nanoparticles. Similarly, the interaction between extract concentration and pH revealed that intermediate extract levels coupled with a pH range of 7.5–8.0 produced nanoparticles with improved size uniformity. The enhanced availability of bioactive compounds under these conditions promoted controlled nucleation and restricted excessive particle growth.

Optimization and Validation of the Design Space

Numerical optimization using the desirability function approach identified the optimum formulation conditions as 0.5336% w/v silver nitrate concentration, 1.35% w/v neem extract concentration, and pH 7.04, with an overall desirability value of 0.937, indicating a highly reliable optimization outcome. The optimized formulation was predicted to produce silver nanoparticles with a particle size of 34.99 nm, zeta potential of −10.0 mV, and a polydispersity index (PDI) of 0.286. To validate the model, the optimized formulation was prepared experimentally and characterized. The observed particle size (36.8 nm), zeta potential (−10.40 mV), and PDI (0.262) were found to be in close agreement with the predicted values. The percentage deviations for particle size, zeta potential, and PDI were 5.17%, 4.00%, and 8.39%, respectively. These low deviation values (<10%) demonstrate the accuracy and predictive capability of the optimization model.

The small particle size obtained is desirable for enhancing surface area and biological activity, while the negative zeta potential indicates acceptable colloidal stability of the nanoparticles. The low PDI value (<0.3) suggests a narrow particle size distribution and good uniformity of the synthesized nanoparticles. Overall, the experimental validation confirmed the robustness of the Quality by Design (QbD)-based optimization approach for the green synthesis of neem-mediated silver nanoparticles.

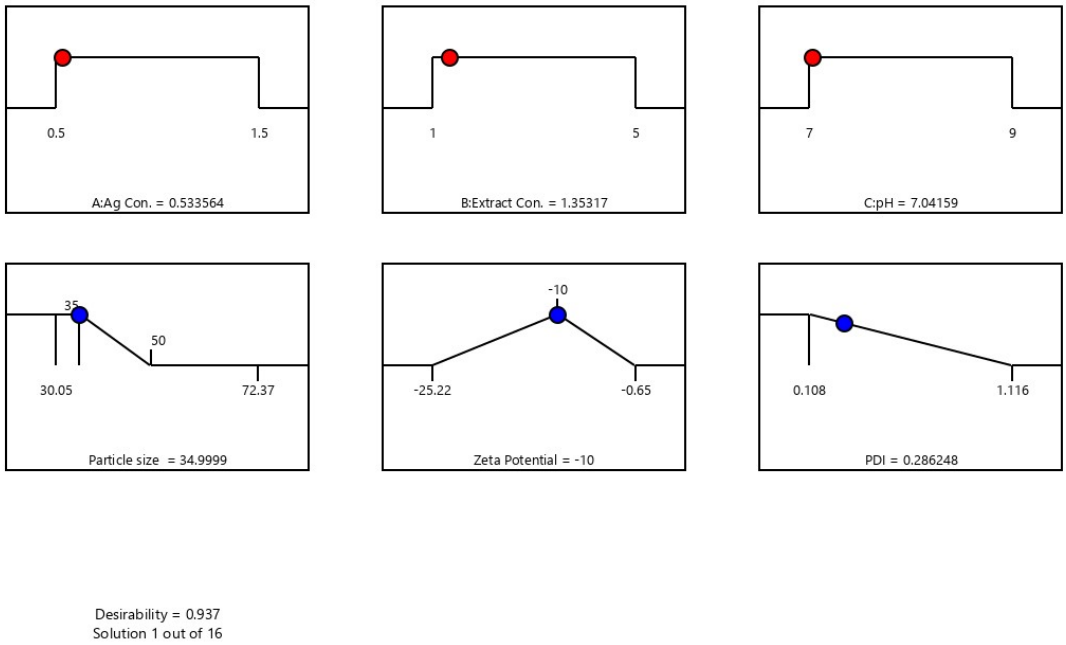

Figure 04. Numerical optimization of Silver Nanoparticles preparation with Desirability value

Table 03: Optimization and Validation of the Design Space for Green Synthesized Silver Nanoparticles

Parameter	Optimized Value / Response	Predicted Value	Observed Value	% Deviation
Silver Nitrate Concentration (% w/v)	0.5336	-	-	-
Neem Extract Concentration (% w/v)	1.35	-	-	-
pH	7.04	-	-	-
Particle Size (nm)	-	34.99	36.8	5.17
Zeta Potential (mV)	-	-10	-10.40	4.00
Polydispersity Index (PDI)	-	0.286	0.262	8.39
Desirability	0.937	-	-	-

The QbD-based optimization successfully identified the critical process parameters governing the green synthesis of neem-mediated silver nanoparticles. Silver nitrate concentration significantly affected particle size and PDI, whereas neem extract concentration predominantly controlled zeta potential. The optimized formulation produced stable nanoparticles with acceptable particle size distribution and surface charge, highlighting the effectiveness of neem extract as a natural reducing and stabilizing agent for eco-friendly synthesis of silver nanoparticles.

Figure 05. Green Synthesis of Silver Nanoparticles Using Neem Leaf Extract and Their SpectroscopicCharacterization

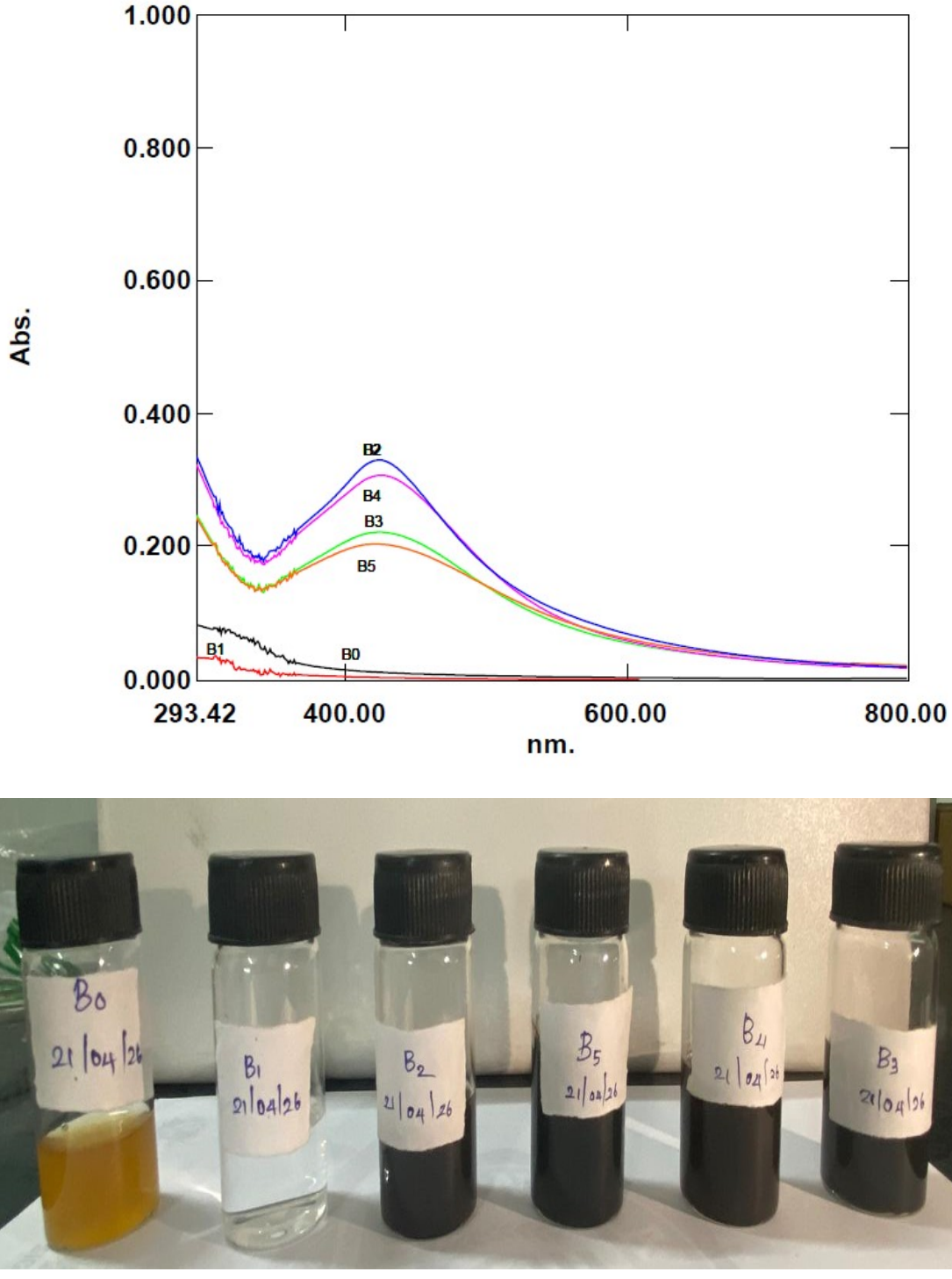

Figure 06. (A) Visual Observation and (B) UV–Visible Characterization of Silver Nanoparticle Synthesis (B0 Neem extract solution, B1 Silver nitrate solution, B2-B5 Silver Nitrate Nanoparticles formation)

The successful synthesis of silver nanoparticles (AgNPs) using neem extract was confirmed through visual observation and UV–Visible spectroscopic analysis. The neem extract solution (B0) exhibited a yellowish-brown color, while the silver nitrate solution (B1) was colorless and transparent. Upon mixing neem extract with silver nitrate solution, the reaction mixtures (B2–B5) gradually changed from light brown to dark brown-black, indicating the reduction of silver ions (Ag^{+}) to metallic silver nanoparticles (Ag^{0}). This color change is a characteristic feature of silver nanoparticle formation and is attributed to the surface plasmon resonance (SPR) phenomenon arising from the collective oscillation of conduction electrons on the nanoparticle surface. The darker coloration observed in samples B2–B5 compared with the control samples further suggested successful nanoparticle synthesis.

The UV–Visible spectra provided additional evidence for AgNP formation. The control samples B0 and B1 showed very low absorbance and lacked a distinct absorption band in the visible region, indicating the absence of nanoparticles. In contrast, samples B2–B5 exhibited prominent absorption peaks in the range of approximately 410–430 nm, which is characteristic of the SPR absorption band of silver nanoparticles. The presence of this peak confirms the reduction of silver ions and the formation of colloidal silver nanoparticles. Among the synthesized samples, B2 showed the highest absorbance intensity (approximately 0.32), indicating the highest concentration of nanoparticles or the most effective reduction process. Sample B4 displayed a slightly lower absorbance intensity, whereas B3 and B5 exhibited comparatively lower absorbance values, suggesting reduced nanoparticle yield. The broadness of the absorption peaks observed for B2–B5 indicates a distribution of particle sizes and possible slight aggregation of nanoparticles. However, the relatively similar peak positions suggest that the synthesized nanoparticles possessed comparable morphological characteristics[29].

The formation of silver nanoparticles can be attributed to the phytochemical constituents present in neem extract, including flavonoids, phenolic compounds, terpenoids, proteins, and reducing sugars. These biomolecules act as reducing agents by converting Ag^{+} ions into metallic Ag^{0} nanoparticles and simultaneously function as capping agents that stabilize the nanoparticles and prevent excessive aggregation. Overall, the observed color change and the characteristic SPR absorption band around 420 nm clearly demonstrate the successful green synthesis of silver nanoparticles using neem extract. The results indicate that neem extract is an effective, eco-friendly, and sustainable reducing and stabilizing agent for the production of silver nanoparticles.

FTIR spectrum of silver nanoparticles

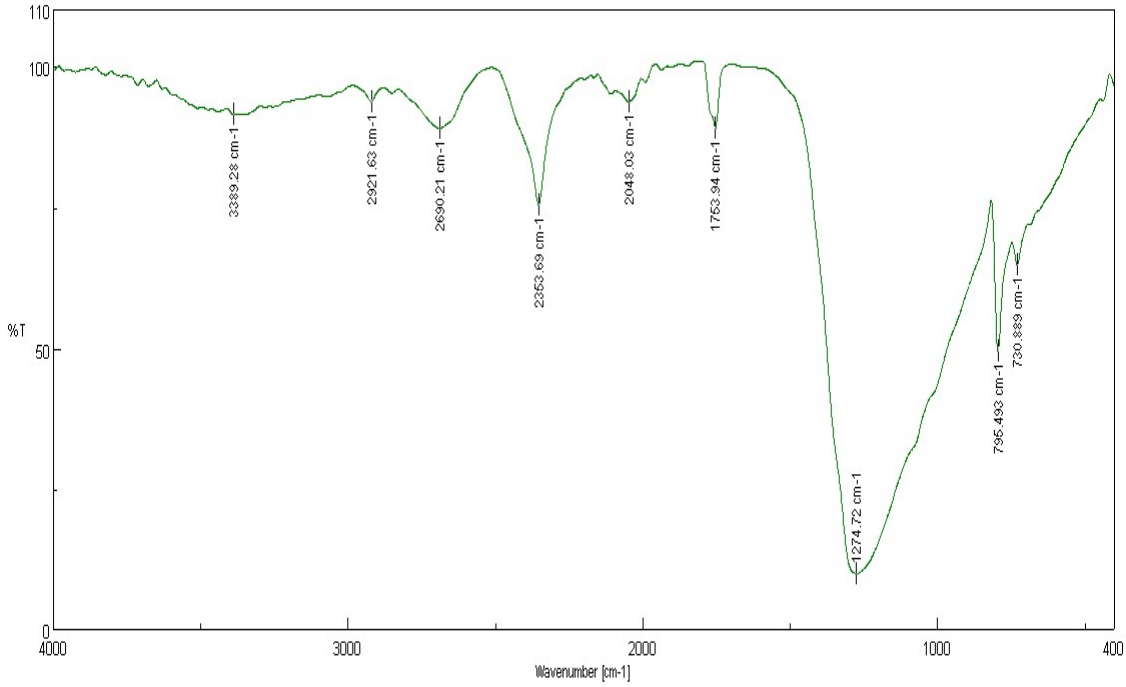

Figure 07. FTIR spectrum of silver nanoparticles synthesized using neem extract

The FTIR spectrum of silver nanoparticles synthesized using neem extract reveals the presence of various functional groups responsible for reduction and stabilization of nanoparticles. A broad peak at ~3338 cm^{-1} corresponds to O–H stretching vibrations of phenols and alcohols, indicating the involvement of polyphenolic compounds from neem extract in the reduction of Ag^{+} ions. The peak at ~2921 cm^{-1} is attributed to C–H stretching of aliphatic groups. The absorption band at ~2630 cm^{-1} may be associated with weak O–H stretching of carboxylic acids, suggesting the presence of acidic phytoconstituents. A peak observed at ~2356 cm^{-1} could be due to atmospheric CO_2 or residual organic compounds. The band at ~2048 cm^{-1} indicates possible C≡C or C≡N stretching, reflecting complex organic interactions during nanoparticle formation. The peak at ~1765 cm^{-1} corresponds to C=O stretching of carbonyl groups, suggesting the role of proteins or flavonoids in capping the nanoparticles. A strong absorption at ~1247 cm^{-1} is assigned to C–O stretching or C–N vibrations, confirming the presence of biomolecules bound to the nanoparticle surface. Peaks at ~795 cm^{-1} and ~770 cm^{-1} correspond to aromatic C–H bending, indicating the presence of substituted benzene rings from plant metabolites. FTIR spectrum confirms that neem extract contains bioactive compounds such as phenols, flavonoids, and proteins, which act as both reducing agents (converting Ag^{+} to Ag^{0}) and capping agents (stabilizing nanoparticles). These functional groups contribute to the formation of stable, biocompatible silver nanoparticles suitable for biomedical applications.

XRD analysis

The XRD pattern of neem-mediated silver nanoparticles exhibited characteristic diffraction peaks corresponding to the face-centered cubic (fcc) structure of metallic silver, confirming successful nanoparticle formation. The prominent peaks indexed to the (111), (200), (220), and (311) planes indicate high crystallinity, with the (111) plane showing dominant intensity, suggesting preferred orientation. Peak broadening observed in the diffractogram reflects the nanoscale size of the particles. The absence of additional impurity peaks confirms the formation of phase-pure silver nanoparticles. These findings demonstrate that neem extract effectively acts as a reducing and stabilizing agent in the green synthesis process, yielding stable, crystalline nanoparticles[30].

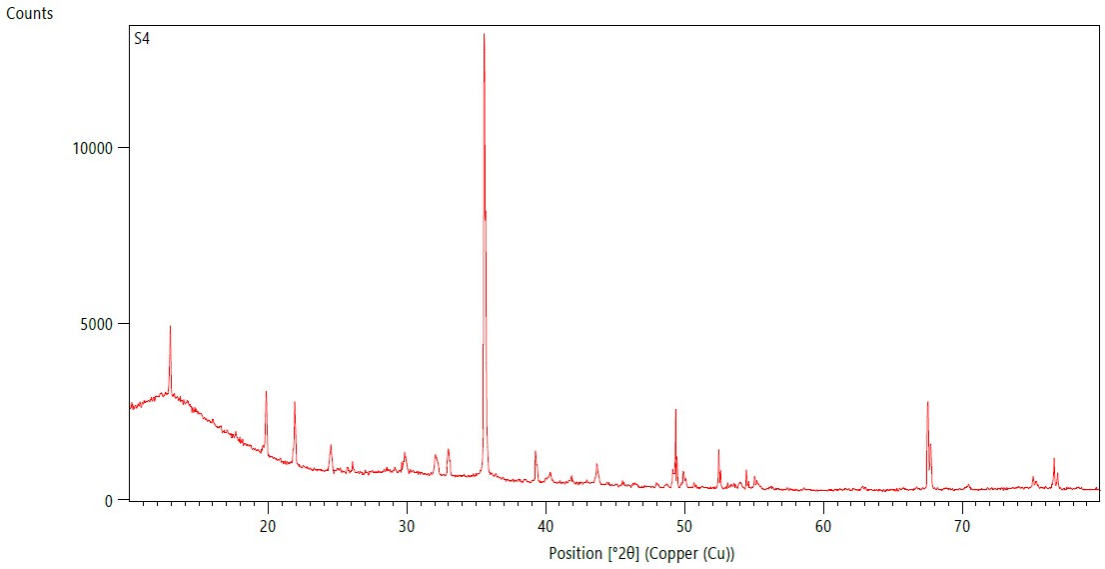

Figure 08. XRD pattern of neem-extract-mediated silver nanoparticles

showing characteristic peaks at 2θ ≈ 38°, 44°, 64°, and 77°, indexed to (111), (200), (220), and (311) planes of face-centered cubic silver.

Particle size and Zeta potential analysis

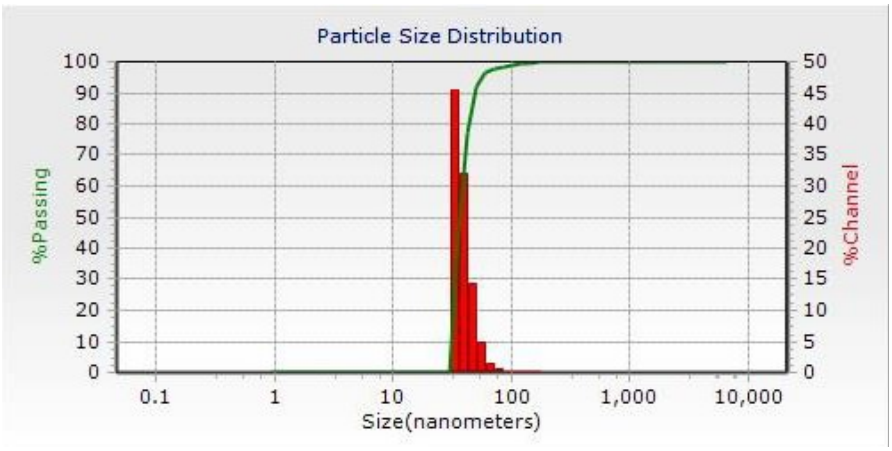

Figure 09. DLS analysis of silver nanoparticles

The DLS analysis of silver nanoparticles synthesized using neem extract shows a single, narrow intensity peak with an average particle size of approximately ~50–100 nm. The polydispersity index (PDI ~1) indicates moderate uniformity and a fairly stable dispersion. The slightly larger size suggests some aggregation and the presence of a phytochemical capping layer from the neem extract.

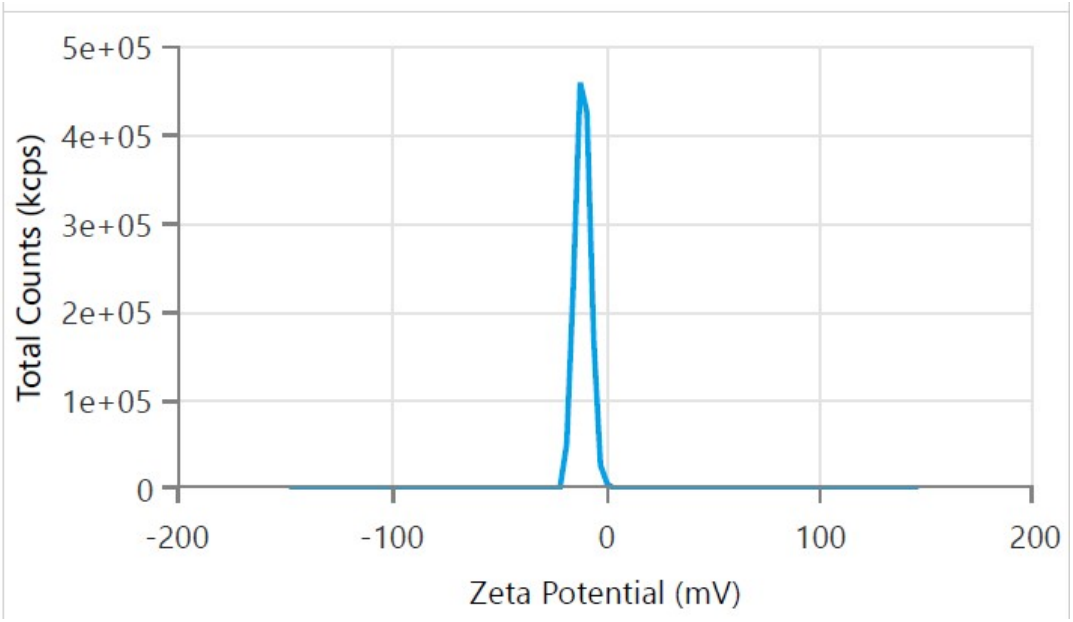

Figure 10. Zeta potential analysis of silver nanoparticles

The zeta potential analysis of silver nanoparticles synthesized using neem extract shows a single, sharp peak centered slightly on the negative side (around ~−10 to −20 mV), indicating that the particles carry a net negative surface charge. This negative zeta potential is attributed to the adsorption of phytochemicals from neem extract (such as flavonoids and phenolic compounds) on the nanoparticle surface, which act as stabilizing agents. The moderately low magnitude of the zeta potential suggests moderate colloidal stability, meaning the nanoparticles are relatively stable but may exhibit some degree of aggregation over time. The result confirms successful capping and stabilization of silver nanoparticles through green synthesis, though the stability is not extremely high.

XRD Analysis of Green-Synthesized Silver Nanoparticle-Loaded Chitosan Hydrogel

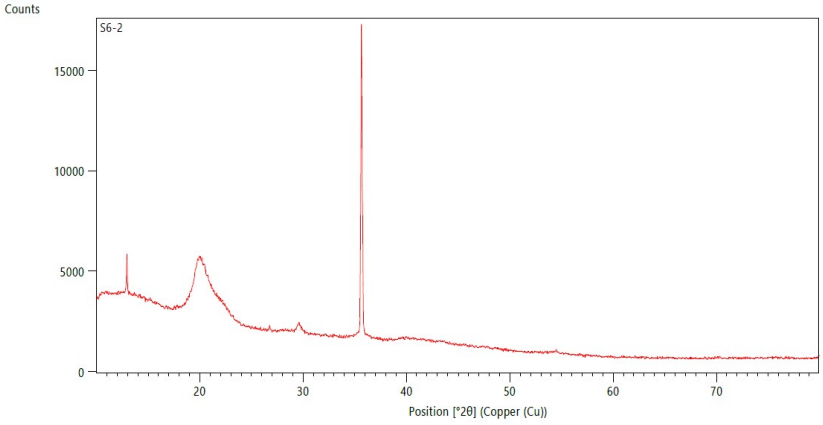

Figure 11. XRD pattern of the green-synthesized silver nanoparticle-loaded chitosan hydrogel

The XRD pattern of the green-synthesized silver nanoparticle-loaded chitosan hydrogel exhibited a prominent diffraction peak at 2θ ≈ 38°, corresponding to the (111) plane of crystalline silver, confirming the successful formation of AgNPs. The broad peak observed around 20–22° is characteristic of the semi-crystalline nature of chitosan. The presence of both chitosan and silver diffraction peaks

indicates the successful incorporation of crystalline AgNPs into the hydrogel matrix. The absence of significant impurity peaks suggests high purity of the synthesized nanoparticles. These results confirm the formation of well-crystalline silver nanoparticles uniformly embedded within the chitosan hydrogel system.

FTIR spectrum of silver nanoparticles incorporated into chitosan hydrogel

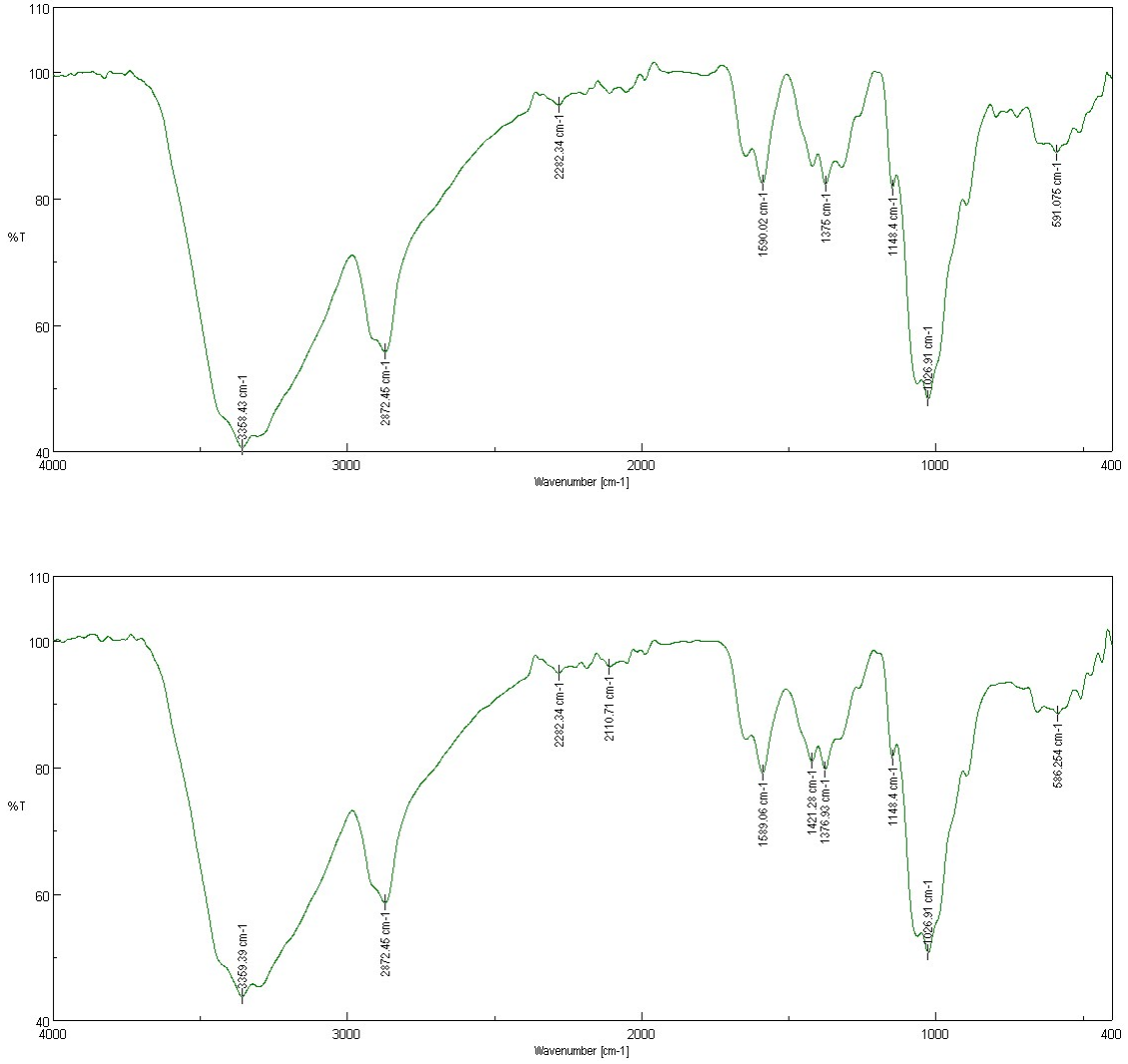

Figure 12. FTIR spectrum of (a) chitosan and (b) silver nanoparticles incorporated into hydrogel

The FTIR spectrum of chitosan shows characteristic peaks confirming its structure. A broad band at ~3358 cm^{-1} corresponds to O–H and N–H stretching, indicating hydrogen bonding. Peaks at 2923 and 2872 cm^{-1} are due to C–H stretching of $–CH_2$ groups. The band at ~1650 cm^{-1} (amide I) suggests residual acetyl groups, indicating partial deacetylation. Peaks at 1375 cm^{-1} (C–N/CH_3 bending), 1148 cm^{-1} (C–O–C bridge), and 1023 cm^{-1} (C–O stretching) confirm the polysaccharide backbone. A peak near 631 cm^{-1} represents out-of-plane vibrations. Overall, the spectrum verifies the presence of chitosan with typical functional groups.

The FTIR spectrum of silver nanoparticles incorporated into a chitosan hydrogel shows the characteristic functional groups of chitosan along with evidence of interaction between the polymer and the nanoparticles. A broad, intense band in the region of ~3500–3200 cm^{-1} corresponds to overlapping O–H and N–H stretching vibrations, indicating extensive hydrogen bonding within the hydrogel network. The peak around ~2870 cm^{-1} is attributed to aliphatic C–H stretching of the chitosan backbone. In the mid-region, the band near ~1589 cm^{-1} is associated with N–H bending (amide II) or amine group vibrations, and its presence and possible

shift suggest coordination between silver nanoparticles and the amino groups of chitosan. Additional peaks at ~1442 and ~1376 cm^{-1} arise from CH_2 bending and C–N stretching or CH_3 deformation vibrations. The strong bands in the range of ~1150–1000 cm^{-1}, including peaks at ~1148 and ~1025 cm^{-1}, correspond to C–O–C glycosidic linkages and C–O stretching, confirming the integrity of the polysaccharide structure. A weaker band around ~686 cm^{-1} may be related to out-of-plane vibrations or weak interactions involving silver. Overall, the spectrum indicates that the chitosan framework is preserved while silver nanoparticles are successfully incorporated, primarily interacting with hydroxyl and amine functional groups.

SEM analysis of silver nanoparticles incorporated into chitosan hydrogel

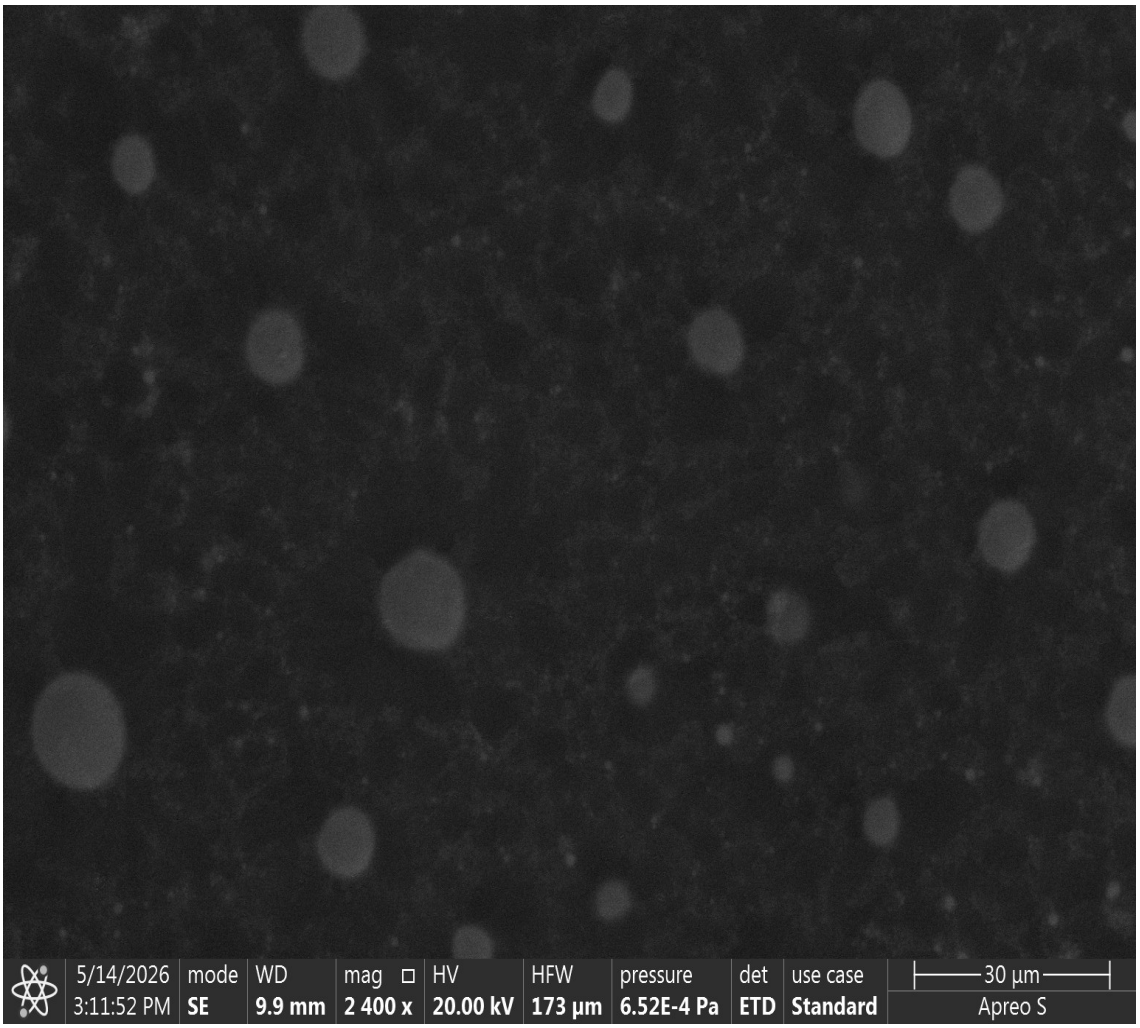

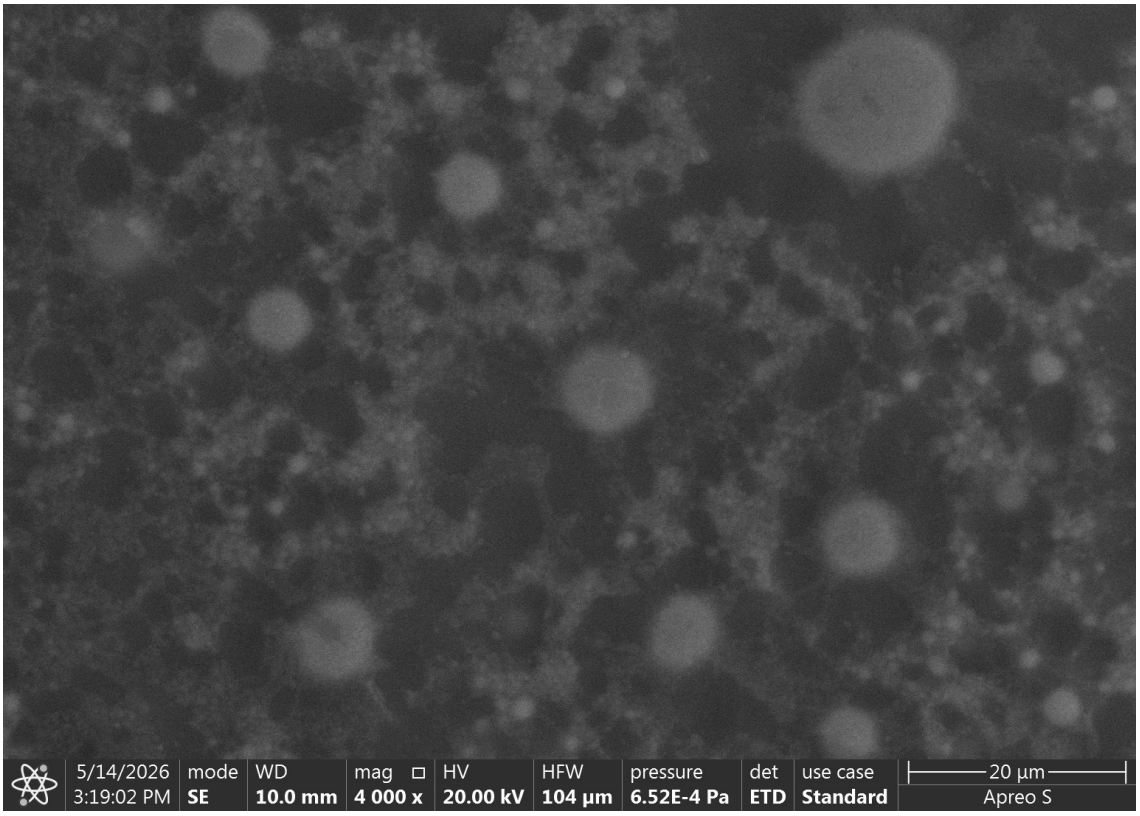

Figure 13. SEM images of silver nanoparticles incorporated into chitosan hydrogel

The surface morphology of the optimized silver nanoparticle (AgNP)-incorporated chitosan hydrogel was examined using scanning electron microscopy (SEM) at magnifications of 2400× and 4000×. The SEM micrographs revealed a relatively rough and porous hydrogel matrix with the presence of numerous spherical particles distributed throughout the polymer network. The bright spherical structures observed in the images are attributed to the embedded silver nanoparticles, indicating their successful incorporation within the chitosan hydrogel. The nanoparticles appeared to be fairly uniformly dispersed with minimal aggregation, suggesting effective stabilization by the chitosan matrix and phytoconstituents present in the neem extract used during green synthesis. The porous architecture of the hydrogel is advantageous for wound-healing applications, as it can facilitate moisture retention, oxygen permeability, and controlled release of silver nanoparticles at the wound site. Furthermore, the homogeneous distribution of AgNPs throughout the hydrogel matrix indicates efficient entrapment and may contribute to sustained antimicrobial activity. SEM analysis confirmed the successful incorporation of silver nanoparticles into the chitosan hydrogel and demonstrated a porous, interconnected structure suitable for wound dressing applications. The observed morphology supports the potential of the developed AgNP-loaded hydrogel as an effective wound-healing system.

CONCLUSION

The present study successfully demonstrated the development and optimization of neem-mediated silver nanoparticles using a Quality by Design (QbD) framework. The Box–Behnken design effectively identified the influence of silver nitrate concentration, neem extract concentration, and pH on the critical quality attributes of the nanoparticles. The optimized formulation produced silver nanoparticles with desirable particle size, acceptable zeta potential, and narrow size distribution, confirming the robustness of the optimization process. Characterization studies including UV–Visible spectroscopy, FTIR, XRD, EDX, and SEM confirmed the successful green synthesis of crystalline silver nanoparticles and their stabilization by phytoconstituents present in neem extract. Furthermore, the incorporation of optimized AgNPs into a chitosan hydrogel resulted in a porous and homogeneous matrix with uniform nanoparticle

distribution. The developed hydrogel system possesses desirable characteristics for topical application and wound management. Overall, the study highlights the potential of QbD-guided green synthesis as an eco-friendly and reproducible strategy for developing silver nanoparticle-based wound-healing formulations.

ACKNOWLEDGEMENT

The authors express their sincere gratitude to the Department of Pharmaceutics, School of Pharmaceutical Sciences, Vels Institute of Science, Technology and Advanced Studies (VISTAS), Pallavaram, Chennai, for providing the necessary facilities and support to carry out this research work.

REFERENCES

1. Basu S, Samanta HS, Ganguly J. Green synthesis and swelling behavior of Ag-nanocomposite semi-IPN hydrogels and their drug delivery using Dolichos biflorus Linn. Soft Mater. 2018;16(1):7–19.
2. Carabineiro S. Applications of gold nanoparticles in nanomedicine: recent advances in vaccines. Molecules. 2017;22(5):857.
3. Roy K, Biswas S, Banerjee PC. Synthesis of Silver nanoparticles by using grape (Vitis vinifera) fruit extract; characterization of the particles and study of antibacterial activity. Research Journal of Pharmaceutical, Biological and Chemical Sciences. 2013 ;4(1):1271–1278.
4. Kaur R, Singh J, Tripathi S. Incorporation of inorganic nanoparticles into an organic polymer matrix for data storage application. Current Appl Phys. 2017;17(5):756–762.
5. Abdal Dayem A, Hossain MK, Lee SB, et al. The role of reactive oxygen species (ROS) in the biological activities of metallic nanoparticles. Int J Mol Sci. 2017;18(1):120.
6. Fukui H. Development of new cosmetics based on nanoparticles. In: Naito M, Yokoyama T, Hosokawa K, Nogi K, editors. Nanoparticle Technology Handbook. 3rd ed. Elsevier; 2018:845–877. ISBN: 978-0-444-64110-6.
7. Bharathi D, Josebin MD, Vasantharaj S, Bhuvaneshwari V. Biosynthesis of silver nanoparticles using stem bark extracts of Diospyros montana and their antioxidant and antibacterial activities. J Nanostruct Chem. 2018;8(1):83–92. doi:10.1007/s40097-018-0256-7.
8. Fathima JB, Pugazhendhi A, Oves M, Venis R. Synthesis of eco-friendly copper nanoparticles for augmentation of catalytic degradation of organic dyes. J Mol Liq. 2018;260:1–8.
9. Sharma P, Bhatt D, Zaidi M, Saradhi PP, Khanna P, Arora S. Silver nanoparticle-mediated enhancement in growth and antioxidant status of Brassica juncea. Appl Biochem Biotechnol. 2012;167(8):2225–2233.
10. Zhang J, Si G, Zou J, Fan R, Guo A, Wei X. Antimicrobial Effects of Silver Nanoparticles Synthesized by Fatsia japonica Leaf Extracts for Preservation of Citrus Fruits. J Food Sci. 2017;82(8):1861–1866.
11. McGillicuddy E, Murray I, Kavanagh S, et al. Silver nanoparticles in the environment: sources, detection and ecotoxicology. Sci Total Environ. 2017;575:231–246.
12. Morones JR, Elechiguerra JL, Camacho A, et al. The bactericidal effect of silver nanoparticles. Nanotechnology. 2005;16(10):2346.
13. Vijayan SR, Santhiyagu P, Ramasamy R, et al. Seaweeds: a resource for marine bionanotechnology. Enzyme Microb Technol. 2016;95:45–57.
14. Patil PS, Kumbhar TS. Antioxidant, antibacterial and cytotoxic potential of silver nanoparticles synthesized using terpenes rich extract of Lantana camara L. leaves. Biochem Biophys Rep. 2017;10:76–81.
15. Jha PK, Jha RK, Rout D, et al. Potential targetability of multi-walled carbon nanotube loaded with silver nanoparticles photosynthesized from Ocimum tenuiflorum (tulsi extract) in fertility diagnosis. J Drug Target. 2017;25:616–625.
16. Sandhiya V, Ubaidulla U. Enhancing cellular uptake and membrane permeability of gallic acid for breast cancer therapy via folate-tagged PEGylated iron oxide nanoparticles as theranostic agent. Bull Natl Res Cent. 2022;46(1):234.
17. Ubaidulla U, Senthilkumar B, Khar RK, Ahmad FJ. Studies on suspension of nimesulide solid dispersion: Development, characterization and in vivo evaluation. Indian J Pharm Sci. 2005;67(4):422-6.
18. John G, Sinha P, Rathnam G, Ubaidulla U, Aravind R. A review on future prospects of niosomes towards drug delivery applications. IOSR J Pharm. 2021;11:1-9.
19. Rama B, Sandhiya V, Swetha M, Rathnam G, Ubaidulla U. Pulsatile drug delivery: A comprehensive review. Int J Pharm Drug Technol. 2015;5(2):125-30.

20. Ubaidulla U, Sinha P, Sangavi T, Rathnam G. Development of silymarin entrapped chitosan phthalate nanoparticles for targeting colon cancer. J Nat Remedies. 2022:659-71.
21. Charumathy A, Ubaidulla U, Sinha P, Rathnam G. Recent update on liposome-based drug delivery system. Int J Curr Pharm Res. 2022;14(3):22-7.
22. Yosef AM, Alqarni RS, Sayd FY, Alhawiti MS, Almahlawi RM, Prabahar K, et al. Preparation and characterization of novel polyelectrolyte liposomes using chitosan succinate layered over chitosomes: A potential strategy for colon cancer treatment. Biomedicines. 2024;12(1):126.
23. Sandhiya V, Ubaidulla U. A review on herbal drug loaded into pharmaceutical carrier techniques and its evaluation process. Futur J Pharm Sci. 2020;6(1):51.
24. Ubaidulla Uthumansha, Sandhiya V, Priyanka Sinha, Exploring nature's pharmacy: breakthroughs in herbal drug development and technology, Futuristic Trends in Pharmacy & Nursing, IIP Series, 6(3), 2024, 282-297.
25. Kumar V V, Saikiran M, Bharathy V R, Ubaidulla U. Formulation Challenges in Dermal Drug Delivery Systems: A Comprehensive Review of Physicochemical Properties and Advanced Delivery Strategies. IJDDT, 14;4,2024.
26. Bharathi Priya, K., Kulathuran Pillai, K., Nalini, C.N. Ubaidulla Uthumansha, Formulation and characterization of 5-fluorouracil and metformin biodegradable nanospheres for treating colon cancer. Futur J Pharm Sci 10, 145 (2024)
27. Padmaja SidramGiram, Swami Shailesh, Omprakash Gadgeppa Bhusnure, Sachin Sivajirao Pandit, Selvaraja Elumalai, Ubaidulla Uthumansha, Jang Hyun Tae & Ganesh Mani. Novel Polyvinyl Alcohol: Polyacrylic Acid Nanofiber Composite for Prolonged Release of Capecitabine: In Vitro and In Vivo Evaluations of Colon-Targeted Drug Delivery. *Fibers Polym* 25, 4665–4676 (2024)
28. Govindarajan M, Rajeswary M, Veerakumar K, et al. Green synthesis and characterization of silver nanoparticles fabricated using Anisomeles indica: mosquitocidal potential against malaria, dengue and Japanese encephalitis vectors. Exp Parasitol. 2016;161:40–47.
29. Jannathul MF, Lalitha P. Apoptotic efficacy of biogenic silver nanoparticles on human breast cancer MCF-7 cell lines. Prog Biomater. 2015;4:113–121.
30. Marslin G, Selvakesavan RK, Franklin G, et al. Antimicrobial activity of cream incorporated with silver nanoparticles biosynthesized from Withania somnifera. Int J Nanomed. 2015;10:5955–5963.